

Steel Corrosion Detection and Quantification Real-Time Using the New Nondestructive Test with Vipulanandan Impedance Corrosion Model

C. Vipulanandan and C. Chockalingam, Center for Innovative Grouting Materials and Technology (CIGMAT) and Texas Hurricane Center for Innovative Technology (THC-IT) - University of Houston.

Copyright 2018, AADE

This paper was prepared for presentation at the 2018 AADE Fluids Technical Conference and Exhibition held at the Hilton Houston North Hotel, Houston, Texas, April 10-11, 2018. This conference is sponsored by the American Association of Drilling Engineers. The information presented in this paper does not reflect any position, claim or endorsement made or implied by the American Association of Drilling Engineers, their officers or members. Questions concerning the content of this paper should be directed to the individual(s) listed as author(s) of this work.

Abstract

Corrosion of steel is a multidimensional process caused by the exposed environments, usage and composition of the material. Also steel is the largest volume of metal used in the construction of oil, gas and water wells, pipelines, piles and storage facilities. Also the corrosion of steel will not only affect the exposed surfaces but also the integrity of the bulk material. On the surface corrosion will be two dimensions (2D). Within the bulk steel, corrosion will be in all directions (3 dimensional-3D) and also not homogenous and hence changes have to be quantified point-to-point or section-by-section to better understand the corrosion processes. Corrosion of steel is a bio-chemo-stress-thermo (BCST) induced parallel and/or series processes (representing the environment and usage) and the corrosion and degradation are very much time depended. Although there are several testing methods such as visual inspection, potential difference, weight change and acoustic monitoring used to detect and quantify corrosion they have many limitations including field applications. Also the current methods cannot quantify the corrosion from section to section in various directions and also separate the surface corrosion from the bulk corrosion.

In this study, a series of experiments were performed to evaluate the steel corrosion using the newly developed non-destructive electrical method using Vipulanandan impedance corrosion model. The potential use of the nondestructive electrical method is to detect and quantify the surface and bulk corrosion separately. The findings from this study indicated the changes in the newly developed electrical corrosion index on the surface and the resistivity in the bulk material. Corrosion of 750 mm (30 in) long steel specimens was studied in 3.5% salt solution for over 500 days. The changes in the specimens were monitored at regular intervals by using the two probes and measuring the impedance-frequency relationship in the frequency range of 20 Hz to 300 kHz. Also the responses were monitored by varying the distances between the two probes. The surface corrosion was quantified using the new electrical corrosion index parameter, which changed from point to point on the surface and at one point it changed from $8.72 \times 10^{-7} \Omega F$ to $2.77 \times 10^{-6} \Omega F$ in 500 days in 3.5% salt solution and the change was 200%. The average changes in the bulk resistivity were over 37,000 (3,700,000%)

compared to less than 1% change in the weight in 10% salt solution in one year.

Introduction

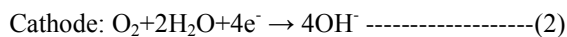
One of the biggest challenges facing the aging infrastructure is the materials loss and deterioration due to corrosion. Many studies indicate that in the US alone, costs due to corrosion loss is more than \$276 billion annually (Michiel et al., 2010). The annual cost of corrosion in the USA oil and gas industry is over \$27 billion and globally \$60 billion. Corrosion is the major cause of deterioration of steel structures and components (Masadeh 2005). Load bearing steel piles are used as foundations for various types of structures and hence corrosion is very much influenced by the environment such as soil, water and soil-water interface. Corrosion of steel pile foundations may result in reduced capacity in the axial and lateral directions. Hence, understanding the rate of steel corrosion is essential to designing the steel based facilities to avoid excessive deflection and failure (Decker et al. 2008; Vipulanandan et al. 2012).

Corrosion is defined as the deterioration of a material because of the continuous bio-chemo-stress-thermo (BCST) reactions with the environment. Practically all environments are corrosive to some degree. For steel, moisture, water, acids, gases, soil, biological activities, thermal cycling and stress variations can cause the degradation of material properties. In the petroleum industry salts, acids, and water are more corrosive than the oil (Fontana, 1987).

Corrosion occurs in unprotected steel structures in any location, and varies in intensity depending on local variables. Accelerated Low Water Corrosion (ALWC) is defined as the localized and aggressive corrosion phenomenon that typically occurs at or below low-water level and is associated with microbially induced corrosion. ALWC corrosion rates are typically 0.5 mm/side/year averaged over time to the point of complete perforation of steel plate. This corrosion process can be significantly affected by bacterial activity and fluctuating water table in addition to the condition of the soil (Cheung et al. 1994 ;Kumar, et al. 2002; Javaherdashti 2005; International Navigation Association, 2005; Zhao et al. 2007; Rozene et al. 2009; Jeffrey, 2009). Marine environments normally

encompass several exposure zones of differing aggressiveness and the corrosion performance of marine structures in these zones requires separate consideration. These zones with the high astronomical tide (HAT) and microbiological activities will contribute to the accelerated low water corrosion (ALWC) (Vipulanandan et al. 2012). Accelerated low water corrosion (ALWC) usually occurs between mean low water springs (MLWS) and low astronomical tide (LAT). Occurrences of ALWC have been noted in the literature as far back as the first half of the 20th century. In view of this history and the presence of ALWC-promoting bacteria in all aquatic environments, commissioning owners would be strongly advised to include ALWC corrosion protection on all maritime structures. Steel corrodes, particularly in a marine environment, through a number of mechanisms that depend on the location of the steel in a structure and other factors. The rate of common 'rusting' corrosion is generally predictable and can be addressed by programming repairs into management systems, but microbial activity is known to contribute to or accelerate corrosion in a number of environments.

To prevent the deterioration mechanisms that affect steel, it is fundamental both to identify and understand the deterioration mechanism that has been the cause of damage. Understanding the deterioration mechanism allows for maintenance that will combat this type of damage. It is widely recognized that the corrosion of carbon steel in soil, water and soil-water interface proceeds according to the following simplified anodic reaction and cathodic reactions in the presence of oxygen and water (Decker et al. 2008).



So the overall chemical reaction is $\text{Fe}_2^{+} + 4\text{OH}^{-} + \text{O}_2 \rightarrow \text{Fe}_2\text{O}_3$ (Rust) + H_2O . When the Fe atoms that leave the surface at the anode as Fe^{2+} move into the environment it forms small pitting holes at the anode. But when the released Fe^{2+} ions remain on the cathodic surface it leads in large depositions of rust at the cathodic surface. These deposits form a hard mass which doesn't have the mechanical strength and is very brittle. The potential of the corroding electrode (anode) with respect to a reference electrode is called corrosion potential. The current that is established because of the corrosion reaction is called the corrosion current and the degree of which directly relates to the rate of corrosion occurring at the surface.

Within the past 10-20 years, there has been growing awareness of an accelerated form of corrosion concentrated around the low-water mark of maritime structures. This Accelerated Low Water Corrosion, or ALWC, is a rapid pitting form of microbial induced corrosion (MIC) that occurs more rapidly than others previously identified. The most common variety of ALWC occurs as a horizontal band around low water, but it can be found occasionally in patches and

extends down to bed level. The appearance and characteristics of ALWC are generally recognizable as lightly adherent orange and black corrosion products over otherwise clean steel.

Methods of Corrosion Detection and Quantification

Corrosion changes the material properties of the metal - decreasing its strength, changing its structure. Hence it is important to be able to detect and evaluate the extent of corrosion of the metal surface. There are many methods that are employed to evaluate corrosion, Visual Inspection, Weight loss measurements, material composition variation, and studies of the structure of the deposition material using XRD measurements. Summary of the current inspection, deterioration and monitoring methods are as follows:

- a) **Visual Inspection:** Here is the easiest type of corrosion detection which is often performed with no complications when there's physical access to the corroded material. The seasoned inspector can determine the kind of corrosion, including general corrosion, pitting corrosion, crevice corrosion, weld and heat affected zone corrosion, erosion corrosion from visual inspection. The amount of corrosion described could be quantified and documented by the use of photos or sketches. For precise measurements of local corrosion penetration by pitting corrosion caused, for instance, numerous kinds of optical or mechanical measuring instruments may be used. But corrosion induced damages and a lot of flaws cannot be inspected for which other techniques that are innovative are used.
- b) **Weight loss measurements:** In this technique, the samples that were corroded are tracked for the variation of its own weight. Together with the lack of substance, its weight falls as the metal corrodes, and so the drop-off in weight over time provides the extent of corrosion. Seica [2000] and Rajani [1996] ran of corroding steel sample, the gravimetric measurements and developed an empirical equation relating the rate of corrosion as well as the weight loss. (Rajani, 1996; Seica, 2000)
- c) **Radiography, ultrasonic and acoustic testing:** These assessments include delivering various types of waves and consequently identify any types of breaks or deformities flaws within the substance. There are lots of restrictions of the kind of recognition techniques as these usually, consider large measurement configurations and may identify just the bodily deformities or breaks in certain kind of alignments. These can't be used to identify deterioration problems which are mainly chemical and result in a lack of physical strength in the place.
- d) **Liquid penetration and leak detection methods:** These processes are employed to detect surface cracks where the surface is coated with specific liquids (paraffin), and penetration is analyzed which

indicates the existence of cracks and used to find the corrosion cracks.

- e) **Electrical methods:** In this method, the electric probes are used to measure the potential drop over the period on the surface by measuring the change in resistance as an outcome of the corrosion and cracks. This helps in finding the crack and flaws as a consequence of corrosion in the metal surface.
- f) **Electrochemical methods:** Each of the methods mentioned above takes substantial quantity of time for detection and measurement and also the majority of them require lab testing where the sample needs to be accumulated in the corrosion website. But in situations where it is impossible to obtain lab samples or in places where the test setup cannot be reached it is impossible to utilize the methods. Consequently, it is important to work with Non-Destructive Testing (NDT) processes for in situ corrosion measurements that offer data quickly and most importantly very precisely. Electrochemical processes evaluate the extent of damage to the metal in corrosive media and solve these issues which are now popular to measure the corrosion. Various electrochemical procedures like the Linear Polarization Resistance (LPR) process, Electrochemical Impedance Spectroscopy (EIS) procedure, and Electrochemical Noise measurements are accustomed to monitoring the corrosion rate of the metallic surface. Polarization measurements are a crucial research tool in investigations of a variety of electrochemical phenomena.

Objectives

The overall objective was to develop and demonstrate the potential of the new nondestructive corrosion detection and quantification method with a new concept of quantifying corrosion using steel specimens. The specific objectives were as follows:

- i. Identify the equivalent electrical circuits for the surface and bulk corrosion of steel and represent them in terms of electrical properties of the material using the impedance frequency relationship.
- ii. Investigate the corrosion of steel specimens with time placed in 10% salt solution and quantify the surface and bulk corrosions along the length of the steel specimens.
- iii. Compare the weight loss due to corrosion with the changes in the electrical properties used to quantify the corrosion.

Materials and Methods

Steel Plates

ASTM A1018 Mild steel was used for this study. For the weight loss study the samples used were 76 mm in length. For the electrical characterization of corrosion, the steel bars used were 750 mm (30 inches) in length and 30 mm width and 4.1 mm in thickness. The chemical composition of the steel is summarized in Table 1.

Salt Solution

For the accelerated test, 3.5% sodium chloride (NaCl) solution was used for corroding the specimens. The steel specimens were placed in this solution in a plastic container for the entire duration (500 days) of testing. The weight loss study was done in 10% salt solution for one year.

THEORY AND CONCEPTS

VIPULANANDAN IMPEDANCE MODEL (Vipulanandan et al. 2013)

Equivalent Circuit

Identification of the most appropriate equivalent circuit to represent the electrical properties of a material is essential to further understand its properties. In this study, an equivalent circuit to represent the surface and bulk corrosion was required for better characterization through the analyses of the impedance spectroscopy data (Vipulanandan et al. 2013-2015). There were many difficulties associated with choosing a correct equivalent circuit. It was necessary somehow to make a link between the different elements in the circuit and the different regions in the impedance data of the corresponding sample. Given the difficulties and uncertainties, researchers tend to use a pragmatic approach and adopt a circuit which they believe to be most appropriate from their knowledge of the expected behavior of the material under study, and demonstrate that the results are consistent with the circuit used.

In this study, different possible equivalent circuits were analyzed to find an appropriate equivalent circuit to represent the smart cement and drilling mud.

Case 1: General Bulk Material – Resistance and Capacitor

In the equivalent circuit for Case 1, the contacts were connected in series, and both the contacts and the bulk material were represented using a capacitor and a resistor connected in parallel (Fig. 1).

In the equivalent circuit for Case 1, R_b and C_b are resistance and capacitance of the bulk material, respectively and R_c and C_c are resistance and capacitance of the contacts, respectively. Both contacts are represented with the same resistance (R_c) and capacitance (C_c) as they are identical. Total impedance of the equivalent circuit for Case 1 (Z_1) can be represented as follows:

$$Z_1(\sigma) = \frac{R_b(\sigma)}{1 + \omega^2 R_b^2 C_b^2} + \frac{2R_c(\sigma)}{1 + \omega^2 R_c^2 C_c^2} - j \left\{ \frac{2\omega R_c^2 C_c(\sigma)}{1 + \omega^2 R_c^2 C_c^2} + \frac{\omega R_b^2 C_b(\sigma)}{1 + \omega^2 R_b^2 C_b^2} \right\}, \quad (3)$$

where ω is the angular frequency of the applied signal. When the frequency of the applied signal was very low, $\omega \rightarrow 0$, $Z_1 = R_b + 2R_c$, and when it is very high, $\omega \rightarrow \infty$, $Z_1 = 0$.

Case 2: Special Bulk Material - Resistance Only

In Case 2, as a special case of Case 1, the capacitance of the bulk material (C_b) was assumed to be negligible (Fig. 2).

The total impedance of the equivalent circuit for Case 2 (Z_2) is as follows:

$$Z_2(\sigma) = R_b(\sigma) + \frac{2R_c(\sigma)}{1 + \omega^2 R_c^2 C_c^2} - j \frac{2\omega R_c^2 C_c(\sigma)}{1 + \omega^2 R_c^2 C_c^2}. \quad (4)$$

When the frequency of the applied signal was very low, $\omega \rightarrow 0$, $Z_2 = R_b + 2R_c$, and when it is very high, $\omega \rightarrow \infty$, $Z_2 = R_b$ (Fig. 3).

In the case of corrosion measurement the two contacts will have different properties and will be represented as shown in Fig. 4 (Vipulanandan Impedance Corrosion Model).

$$Z = R_b + \frac{R_c}{1 + \omega^2 R_c^2 C_c^2} + \frac{R_i}{1 + \omega^2 R_i^2 C_i^2} - j \left(\frac{\omega R_c^2 C_c}{1 + \omega^2 R_c^2 C_c^2} + \frac{\omega R_i^2 C_i}{1 + \omega^2 R_i^2 C_i^2} \right) \quad (5)$$

Case 2 equivalent circuit was used to determine the contact electrical resistance (R_c) and contact capacitance (C_c) at the surface between steel bar and the probe. During the impedance characterization at least 15 data were collected during each test and the data was used to determine the five unknowns in Eqn. (5)

The resistance (R) and capacitance (C) for the bulk material between two points are defined as:

$$R = \rho \frac{L}{A} = \rho K \quad (6)$$

$$C = \epsilon \frac{A}{L} \quad (7)$$

where A = cross-sectional area, L = distance between the two probes, ρ = resistivity of the material, ϵ = absolute permittivity of the material

The product of equations given in (6) and (7) results as

$$RC = \rho \epsilon \quad (8)$$

Since ρ and ϵ in equations (6) and (7) are material properties, hence RC at the point of contact is also material property, will be referred as electrical corrosion index. This parameter can be used in characterizing the surface corrosion.

Steel Electrical Resistivity

The electrical resistivity of uncorroded steel (ρ_0) is $1.59 \times 10^{-7} \Omega\text{m}$ (Giancoli, 1995). Based on the resistance measured for uncorroded steel (R_0) at high frequency (300 kHz) using the two probes (Contact 1 and 2) and using the uncorroded resistivity of steel (ρ_0) in Eqn. (6) the parameter K was determined. Eqn. (6) with the parameter K was used to determine the resistivity of steel with time ($\rho(t)$) by measuring the corresponding bulk resistance ($R(t)$). Also the changes in corroding steel electrical resistivity ($\Delta\rho(t)$) was calculated using the equation (9) and change in the bulk resistance measured $\Delta R(t)$. Hence the percentage change in resistance will directly related to the percentage change in resistance. Also the resistivity at any time ($\rho(t)$) can be obtained by using Eqn. (10).

$$\Delta\rho(t)/\rho_0 = \Delta R(t)/R_0 \quad (9)$$

$$\rho(t) = \rho_0 + \Delta\rho(t) \quad (10)$$

Results and discussion

Weight Loss Method (ASTM G1)

Steel samples with a dimension of about $76 \text{ mm} \times 30.54 \text{ mm} \times 4.14 \text{ mm}$ were used for this experiment. Specimen was placed in 10% sodium chloride solution and tested regularly. At every cycle, weight and dimension of the specimen were measure using a Vernier caliper. According to ASTM G1-90 standard, the specimens were cleaned and weight and dimensions were measured to estimate the corrosion rate.

As shown in Figure 6 the weight of the corroding steel specimen reduced from 812.1 g to 803.6 g in 1 year of corrosion. The corrosion rate varied with time and the average was about $3.8 \times 10^{-7} \text{ mm/year}$.

Electrical Method

The impedance-frequency measurements were performed on a weekly basis for 500 days. The frequency range used was from 20 Hz to 300 kHz. The observed shape of the curve represents the Case 2 in Figure 3 indicating that the bulk material can be represented as the resistance (inner layer of steel), the surface of the steel (outer layer) as a parallel combination of resistance and capacitance. The total impedance of the corroding steel increased continuously with time.

The changes in the bulk resistances (R_b) measured with various distances (8 inches, 16 inches and 24 inches) and time are shown in Figure 8. Although resistance is not a material property, the percentage change in resistance will be directly related to the percentage change in resistivity (Eqn (9)).

For 8 inches distance measurement, average bulk resistance increased from 0.111Ω (R_0) to 4160Ω ($R(t)$) in 500 days of corrosion study, which showed a change of 37,484 times increase in the resistance and also the electrical resistivity. This also reflects the corrosion inside the steel specimen along the length of the specimen. Similarly for 16 inches distance measurement, bulk resistance increased from 0.124Ω to 5042Ω , which shows a change of 40,492 times increase in the resistance and also the electrical resistivity. Also for 24 inches distance measurement, bulk resistance increased from 0.131Ω to 5810Ω , which shows a change of 44,340 times increase in the resistance and also the electrical resistivity. All these changes indicate that inner layer of steel is also corroding which would not be reported by the other corrosion experiments which are done. As rust is an oxide compound, with an increase in corrosion or rust formation, the resistance and resistivity of the material increased with time.

Bulk Resistivity

The resistivity of the corroding Steel specimen measured using nondestructive corrosion sensing technique is shown in Figure 9 for the testing time period of 500 days. The resistivity of the material was calculated using the equations (9) and (10). The resistivity of the steel increased from $1.59 \times 10^{-7} \Omega\text{m}$ to $5.96 \times 10^{-3} \Omega\text{m}$ for length of 8 inches, a change of 37,484 times higher. For 16 inches length along the test specimen the resistivity increased from $1.59 \times 10^{-7} \Omega\text{m}$ to $6.47 \times 10^{-3} \Omega\text{m}$, a change of 40,492 times higher. For 24 inches of length along the test specimen the average resistivity increased from $1.59 \times 10^{-7} \Omega\text{m}$ to $7.05 \times 10^{-3} \Omega\text{m}$, a change of 44,340 times higher for length of 24 inches for a testing period of 500 days, which clearly indicates the corrosion level in the bulk material. Also the electrical resistivity change with the length indicating non-uniform corrosion within the bulk material along the length.

Surface Characterization

The resistance of the contact 1 which was kept as a constant measurement contact for all the three distance (length =8, 16, 24 Inches) is shown in Figure 10 for the testing time period of 500 days. It was observed that the measured contact resistance increased with time for all the specimens but only results of one specimen is discussed. The higher resistance values of at the Contact #1 indicated that the steel is corroding and reacting with the corrosive environment. The resistance value at contact #1 increased from 0.06Ω to 6964Ω during the testing period of 500 days, which indicated the corrosion level was high (Figure 10). The variation of resistance of the contact #2 points are shown in Figure 11 for the testing time period of 500 days. It could be observed that the steel specimen's contact resistance increased with time. The higher resistance value of the three Contact #2 points over Contact #1 indicated the steel specimen was corroding more compared to Contact #1.

It could also be noted that resistance value at various contact points were different because it was observed that corrosion observed (visual) at contact #2 at 24 inches from

contact #1 was higher corrosion than 16 inches the contact #2. Also contact #2 corrosion at 16 inches had higher corrosion product than 8 inches as shown in Figure 7. As it could be seen in Figure 7 (visual observation) that the 24 inches contact #2 had a crack with a very loose surface layer, which indicated it is more corroded, 16 inches contact place had a corrosion pit and 8 inches had a smooth rust layer. This makes the nondestructive electrical corrosion sensing method very sensitive. Resistance value of the contact #2 at 8 inches increased from 0.07Ω to 7322Ω during the testing period of 500 days (Figure 11). The contact resistance increased from 0.07Ω to 8658Ω during the testing period of 500 days for contact #2 at 16 inches and 0.07Ω to 10388Ω during the testing period of 500 days for contact #2 at 24 inches which indicated the corrosion level was highest at this location.

Contact Capacitance

The variation of capacitance at the contact #1 on the steel surface (C_{C1}) is shown Figure 12. It can be observed that the contact capacitance of the contact #1 decreased with increasing corrosion time hence the capacitance material decreased with corrosion as resistance builds up. This study gives us a clear idea about the relationship between capacitance and corrosion. The change in capacitance value of the contact #1 indicated the steel specimen is corroding, whereas there was much difference with three Contact #2 as it was corroding more as compared to Contact #1 surface. This difference in both the contacts indicates not only corrosion but also the accuracy of the method to separate both the contacts precisely. The capacitance value of the contact #1 of the steel surface decreased from $5.41 \text{ E-}09 \text{ F}$ to $2.61 \text{ E-}09 \text{ F}$ during the testing period of 500 days, decrease of 95%, which indicated the corrosion level was high.

The variation of capacitance at the contact #2 points on the steel surface (C_{C2}) is shown in Figure 13. It can be observed that the contact capacitance of the contact #2 decreased with increasing corrosion period. Higher change was observed with Contact #2 capacitance as it was corroding more is compared to Contact #1 surface. Capacitance value of the contact #2 at 8 inches of the steel surface decreased from $1.58 \text{ E-}09 \text{ F}$ to $3.06 \text{ E-}10 \text{ F}$ during the testing period of 500 days, 81% decrease. At contact #2 at a distance 16 inches the capacitance decreased from $1.22 \text{ E-}09 \text{ F}$ to $2.82 \text{ E-}10 \text{ F}$ during the testing period of 500 days, 77% decrease. At contact #2 at a distance 24 inches measurement the capacitance decreased from $1.03 \text{ E-}09 \text{ F}$ to $2.67 \text{ E-}10 \text{ F}$ during the testing period of 500 days, 74% decrease.

Electrical Corrosion Index

The electrical corrosion index was defined as the product of resistance and capacitance $R \cdot C$, for the corroding steel specimen at contact 1 in 3.5% NaCl solution is shown in Figure 14. From the figure, the rust material on the surface of the corrosion index for steel increased with time, which clearly indicated the degradation of steel.

As rust is an oxide compound, with an increase in corrosion or rust formation, the resistance and resistivity of the

material start to increase, by which we obtain this result. The higher $R_c C_c$ value of the Contact 1 indicated that the steel specimen is corroding, whereas there is much difference with Contact 2 as corrosion is even higher. This difference in both the contacts indicates not only corrosion but also the accuracy of the method to separate both the contacts material properties and denote its characteristics. $R_{C_1} C_{C_1}$ value of the steel specimen increased from $1.51 \text{ E-}06 \text{ } \Omega\text{F}$ to $1.82 \text{ E-}05 \text{ } \Omega\text{F}$ in a testing period of 500 days, which indicated the steel has corroded over 11 times (1100%).

$R_{C_2} C_{C_2}$ value for the contact#2 at 8 inches increased from $5.97 \text{ E-}07 \text{ } \Omega\text{F}$ to $2.24 \text{ E-}06 \text{ } \Omega\text{F}$ in a testing period of 500 days, an increase of 275%. The $R_{C_2} C_{C_2}$ value for the contact#2 at 16 inches increased from $7.57 \text{ E-}07 \text{ } \Omega\text{F}$ to $2.44 \text{ E-}06 \text{ } \Omega\text{F}$ in a testing period of 500 days, an increase of 222%. The $R_{C_2} C_{C_2}$ value for the contact#2 at 24 inches increased from $8.72 \text{ E-}07 \text{ } \Omega\text{F}$ to $2.77 \text{ E-}06 \text{ } \Omega\text{F}$ in a testing period of 500 days, an increase of 218%. It could be noted that $R_{C_2} C_{C_2}$ values increased with time but the change was much less than that was observed for the bulk material.

Conclusions

In this study, a new method was used to detect and quantify surface and bulk corrosion steel in 3.5% salt solution. Also the weight loss of steel in 10% salt solution was investigated for one year. A mathematical model was developed to model the Impedance-frequency data from the experiments to obtain the bulk resistance, contact resistance (R_c) and capacitance (C_c), and the electrical corrosion index $R_c C_c$. Based on the corrosion of steel was monitored for 500 days in 3.5% solution with the changes in the electrical properties, following conclusions can be deduced:

1. The weight loss in the steel in 10% salt solution for one year was less than 1%.
2. Steel specimen which was subjected to marine corrosion (3.5% salt solution) for a period of 500 days, the resistivity of the steel specimen increased from $1.59 \times 10^{-7} \text{ } \Omega\text{m}$ to $5.96 \times 10^{-3} \text{ } \Omega\text{m}$ for measurement length of 8 inches, $1.59 \times 10^{-7} \text{ } \Omega\text{m}$ to $6.47 \times 10^{-3} \text{ } \Omega\text{m}$ for measurement length of 16 inches and $1.59 \times 10^{-7} \text{ } \Omega\text{m}$ to $7.05 \times 10^{-3} \text{ } \Omega\text{m}$ for measurement length of 24 inches in a testing period of 500 days. The changes in the bulk resistivity were over 37,000 (3,700,000%) compared to less than 1% change in the weight in 10% salt solution in one year
3. The electrical corrosion index $R_c C_c$ for contact #1 increased due to corrosion of the steel, the $R_{C_1} C_{C_1}$ of the steel specimen increased from $1.51 \text{ E-}06 \text{ } \Omega\text{F}$ to $1.82 \text{ E-}05 \text{ } \Omega\text{F}$. the steel has corroded over 11 times (1100%) compared to the uncorroded index.
4. The electrical corrosion index $R_c C_c$ for contact #2 also increased due to corrosion of the steel, the

$R_{C_2} C_{C_2}$ of the steel specimen increased from $5.97 \text{ E-}07 \text{ } \Omega\text{F}$ to $2.24 \text{ E-}06 \text{ } \Omega\text{F}$ for contact #2, 8 inches from contact#1, 275% increase. The $R_{C_2} C_{C_2}$ increased from $7.57 \text{ E-}07 \text{ } \Omega\text{F}$ to $2.44 \text{ E-}06 \text{ } \Omega\text{F}$ for contact #2, 16 inches from contact#1, 222% increase. The $R_{C_2} C_{C_2}$ increased from $8.72 \text{ E-}07 \text{ } \Omega\text{F}$ to $2.77 \text{ E-}06 \text{ } \Omega\text{F}$ for contact #2, 16 inches from contact#1, 218% increase. The change in the electrical corrosion index was over 2 times or 200% compared to the uncorroded index.

5. A material property which characterized the surface corrosion was determined to be as the product of resistance and capacitance.
6. The percentage change in the bulk electrical resistivity was much higher than the changes observed on the surface represented by the corrosion index change.
7. Vipulanandan impedance corrosion model was effective in characterizing the bulk and surface corrosion using the two probe method.
8. Since the material degradation affects the microstructure of the material and other properties, the electrical method is a very sensitive method for monitoring the steel degradation.

Acknowledgements

This study was supported by the Center for Innovative Grouting Materials and Technology (CIGMAT) and Texas Hurricane Center for innovative Technology (THC-IT) at the University of Houston, Houston, Texas.

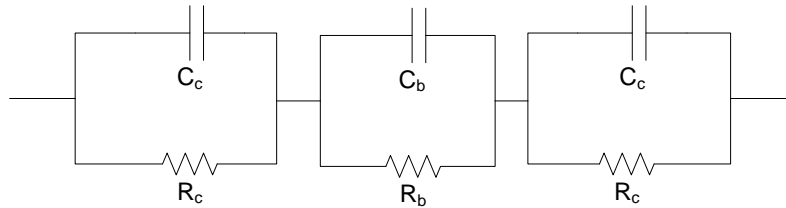
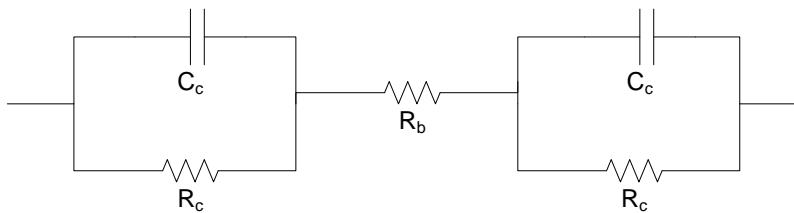
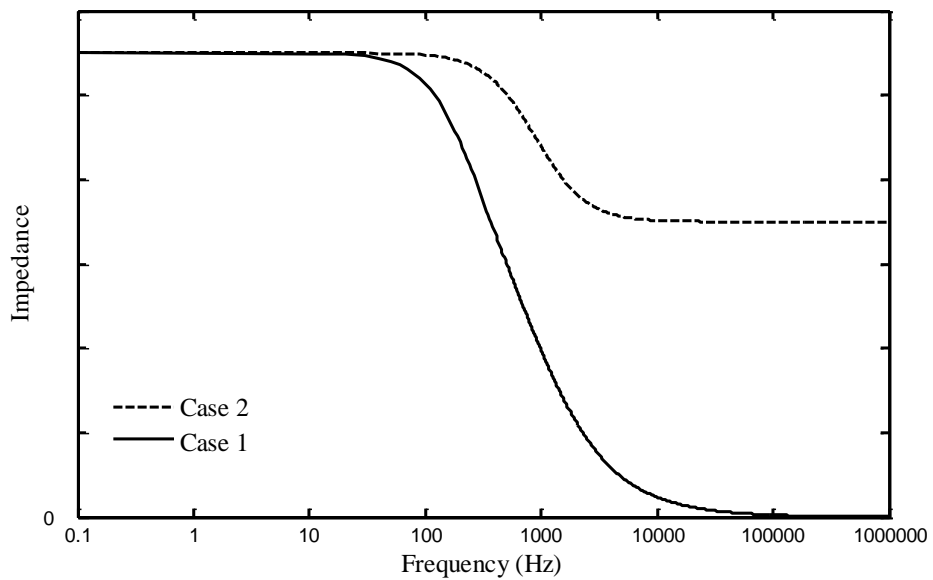
References

1. Ahmad, Z., Hwa K., Chai, Dimitrios G. (2015). "Non-Destructive Evaluation for Corrosion Monitoring in Concrete: A Review and Capability of Acoustic Emission Technique" Sensors.
2. ASTM D5868-95. Standard Test Method for Lap shear Adhesion for Fiber Reinforced Plastics(FRP) Bonding. Annual Book of ASTM Standards, West Conshohocken, Philadelphia.
3. ASTM A 36/A 36M – 04 Standard Specification for Carbon Structural Steel, Annual Book of ASTM Standards, West Conshohocken, Philadelphia.
4. ASTM D1141-98, "Standard Practice for the Preparation of Substitute Ocean Water", ASTM Standard.
5. ASTM G1-90, "Standard Practice for Preparing, Cleaning, and Evaluating Corrosion Test Specimens", ASTM Standards, West Conshohocken, Philadelphia.
6. ASTM G31-72, "Standard Practice for Laboratory Immersion Corrosion Testing of Metals", ASTM Standards, West Conshohocken, Philadelphia.
7. Chiew, S.P., Yu, Y. and Lee C.K. (2011) "Bonding failure of steel beams strength with FRP laminates-Part 1", Journal of

- Constructional Steel Research 66, pp. 1047-1056.
8. Cheung, C.W.S. and Walsh, F.C. et al (1994) "Microbial Contributions to the Marine Corrosion of Steel Piling." International Biodeterioration & Biodegradation, 259-274.
 9. Cutnell, J. and Johnson, K. (1995). "Physics" 3rd Edition, pp 345.
 10. Davis, J.R. (2000). "Corrosion: Understanding the Basics.", Vol.1, pp. 223-254.
 11. Decker, J. B., Rollins, K. M. and Ellsworth, J. C. (2008). "Corrosion Rate Evaluation and Prediction for Pile Based on Long-Term Field Performance." Geotechnical and Geoenvironmental Engineering, 341-351.
 12. Fontana, Mars G., "Corrosion Engineering" 3rd ed, McGraw-Hill, 1987.
 13. Giancoli, D.C. (1995). "Physics: Principles with Applications.", Vol.1, pp 127.
 14. Hamdy, A.S., Shenawy, E.E. and Bitrar, T.E., (2006), "Electrochemical Impedance Spectroscopy Study of the Corrosion Behavior of Some Niobium Bearing Stainless Steels in 3.5% NaCl," Int. J. Electrochem. Sci., 1, pp. 171-180.
 15. Hilbert, L.R. (2006). "Monitoring corrosion rates and localised corrosion in low conductivity water," Corrosion Science, Vol. 48, No. 12, Dec 2006, pp. 3907-3923.
 16. Javaherdashti, R. (2005). "Microbiological contribution to accelerated low water corrosion of support piles." Australasian Corrosion Conference.
 17. Jeffrey, R. and Melchers, R. E. (2009). "Corrosion of vertical mild steel strips in sea water", corrosion science 51, 2291-2297.
 18. Jothilakshmi, N., Nanekar, P., Kain, V. (2013). "Assessment of Intergranular Corrosion Attack in Austenitic Stainless Steel Using Ultrasonic Measurements." Corrosion.
 19. Kamaitis, Z., (2008). "Modelling of Corrosion Protection for Reinforced Concrete Structures with Surface Coatings," Journal of Civil Engineering and Management, 14(4), pp. 241-249
 20. Kumar, A., Stephnson, L. D. (2002). "Accelerated Low Water Corrosion of Steel Piling in Seawater." 30th International Navigation Congress.
 21. Krebs, L.A. (2003). "A Brief history of corrosion sensing methods." Corrosion
 22. Masadeh, S. (2005). "Electrochemical Impedance Spectroscopy Of Epoxy-Coated Steel" Journal of Minerals and Materials Characterization and Engineering, Vol. 4 No. 2, 2005, pp. 75-84.
 23. McCafferty, E.(2010). "Introduction to Corrosion Science." Vol.1, pp. 21-23.
 24. Mirtaheri, P., Grimnes, S.(2005), " Electrode Polarization Impedance in Weak NaCl Aqueous Solutions," IEEE Transaction on Biomedical Engineering, Vol.52., No.12.
 25. Michiel P.H., Brongers CC, Gerhardus HK, Neil G (2010). Technologies and NACE. <http://www.corrosioncost.com/prodmanu/idex.htm>.
 26. Popova, A., Sokolova, E. Raicheva, S. and Christov, M., (2004) AC and DC study of the temperature effect on mild steel corrosion in acid media in the presence of benzimidazole derivatives, Corrosion Science 45 (2003), pp. 33-58.
 27. Rajani, B., Zhan, C., Kuraoka, S. "Pipe Soil Interaction analysis of Joined water mains," Canadian Geotechnical Journal. 33, 393-404, 1996.
 28. Rebak, R.B., Xia, Z., Safruddin, R. and Szklarska-Smialowska, Z., (1995) "Electrochemical Processes Controlling SCC of Underground Pipelines", Paper No. 184, Paper presented at NACE International's Corrosion 95 Annual Conference.
 29. Roberge, P. R., York San Francisco Washington, N., (1999). "Handbook of Corrosion Engineering." Vol.1, pp. 4.
 30. Sankara, P. (2014). "Corrosion Control in the Oil and Gas Industry." Vol.1, pp.5.
 31. Seica, M.V and Packer, J.A. (2000) "Mechanical Properties and strength of aged Cast Iron pipes," Journal of materials in Civil Engineering, ISSN 0899-1561, 2000.
 32. Song, H.W. and Saraswathy, V., (2007) "Corrosion monitoring of reinforced concrete structures — a review." Int. J. Electrochem. Sci. 2007, No. 2, pp. 1-28.
 33. Swain, G.W. (1996) "OCE -4518 Protection of Marine Materials Class Notes", Florida Institute of Technology.
 34. Townsend, H. E. (1996). "Behavior of Painted Steel and Aluminum Sheet in Laboratory" Corrosion.
 35. Vipulanandan, C. and Pan, D. (2012) "Repair Methods for Corroded Steel Piles" Proceedings, Deep Foundation Institute, CD, October 2012.
 36. Vipulanandan, C. and Prashanth, P. (2013). "Impedance Spectroscopy Characterization of A Piezoresistive Structural Polymer Composite Bulk Sensor," Journal of Testing and Evaluation, Vol. 41, No. 6, pp. 898-904.
 37. Vipulanandan, C., and Mohammed, A., (2015) "Smart Cement Modified With Iron Oxide Nanoparticles to Enhance the Piezoresistive Behavior and Compressive Strength for Oil Well Applications." Journal of Smart Materials and Structures, Vol. 24 Number 12, pp. 1-11.
 38. Whitney, W.R. (1903). "The Corrosion of Iron." J.Am.Chem.Soc.
 39. Yuan, X., Sun, D.B., Yu, H.Y. and Wang, Y. (2009). "Effect of nono-SiC particles on the corrosion resistance of NiP-SiC composite coatings," International Journal of Minerals, No. 4, pp.444.
 40. Zaki, A. (2006). "Principles of Corrosion Engineering and Corrosion Control." Vol.1, pp.1.
 41. Zelinka, S.L., Stone, D.S. and Rammer, D.R. (2007). "Equivalent Circuit Modeling of Wood at 12% Moisture Content." Wood and Fibre Science, 39(4), pp. 556-565.
 42. Zhao, X. and Duan, J. et al (2007). "Effect of Sulfate-Reducing Bacteria on Corrosion Behavior of Mild Steel in Sea Mud". J. Mater. Sci. Technol., Vol. 23, pp323-327.

Table 1 Chemical Composition of Type A1018 M Carbon Steel

Iron (Fe) (%)	Carbon (C) (%)	Manganese (Mn) (%)	Phosphorus (P) (%)	Sulfur (S) (%)
98.81 - 99.26	0.18	0.6 - 0.9	0.04	0.05

**Figure 1. Equivalent circuit for Case 1****Figure 2. Equivalent circuit for Case 2****Figure 3. Comparison of typical responses of equivalent circuits for Case 1 and Case 2**

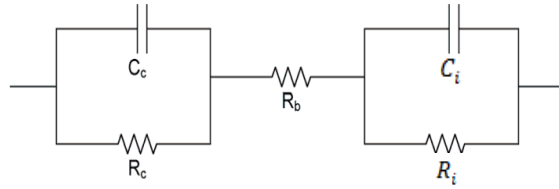


Figure 4. Vipulanandan Impedance Corrosion Model for the Two Probe Measurement (Case 2)

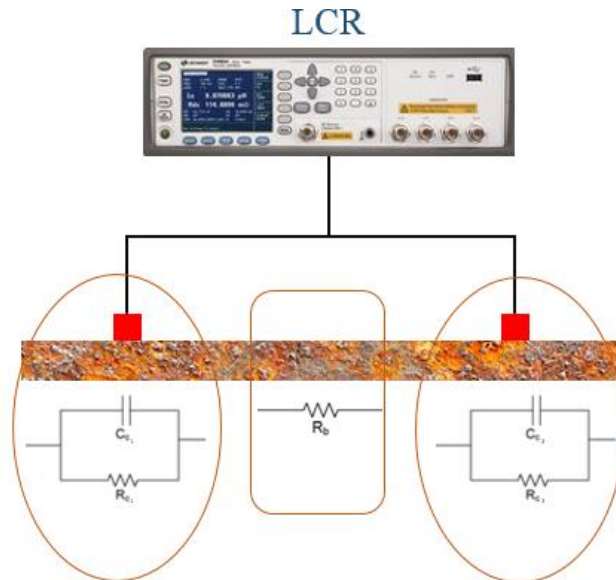


Figure 5. Electrical representation of Nondestructive Electrical testing

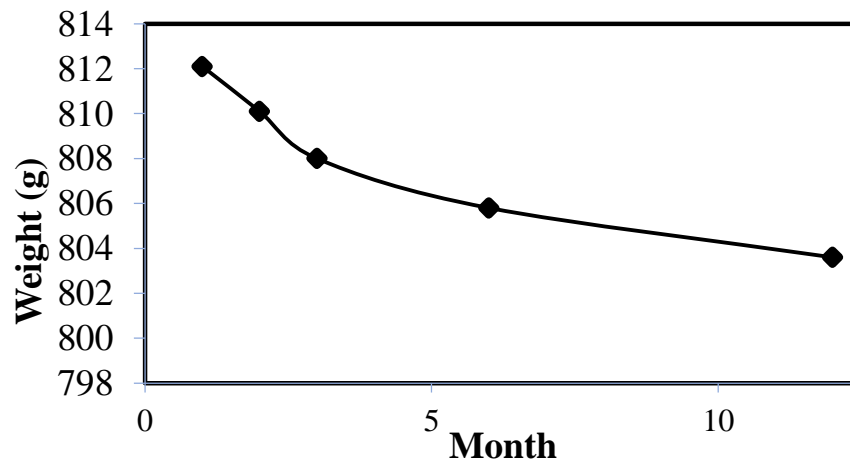


Figure 6. Weight of the Corroding specimen with Time in 10% NaCl Solution

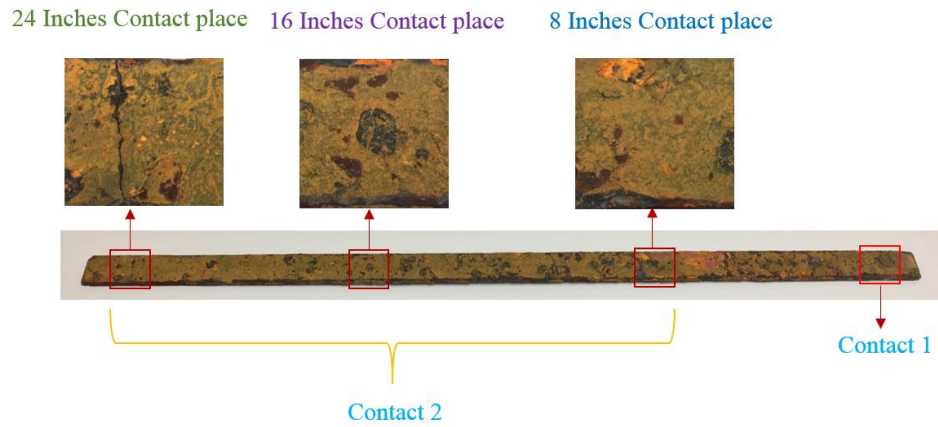


Figure 7. Visual Inspection of Surface Corrosion of Steel Specimen Corroded in 3.5% NaCl solution for a testing period of 1 Year

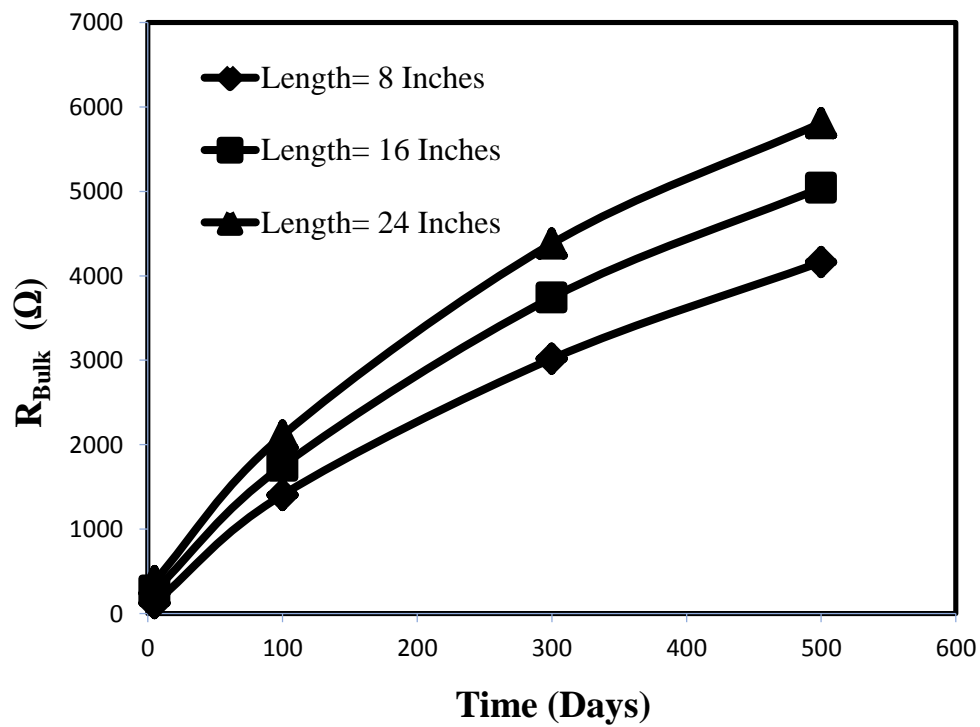


Figure 8. Variation of Bulk Resistance with Time in 3.5% NaCl Solution

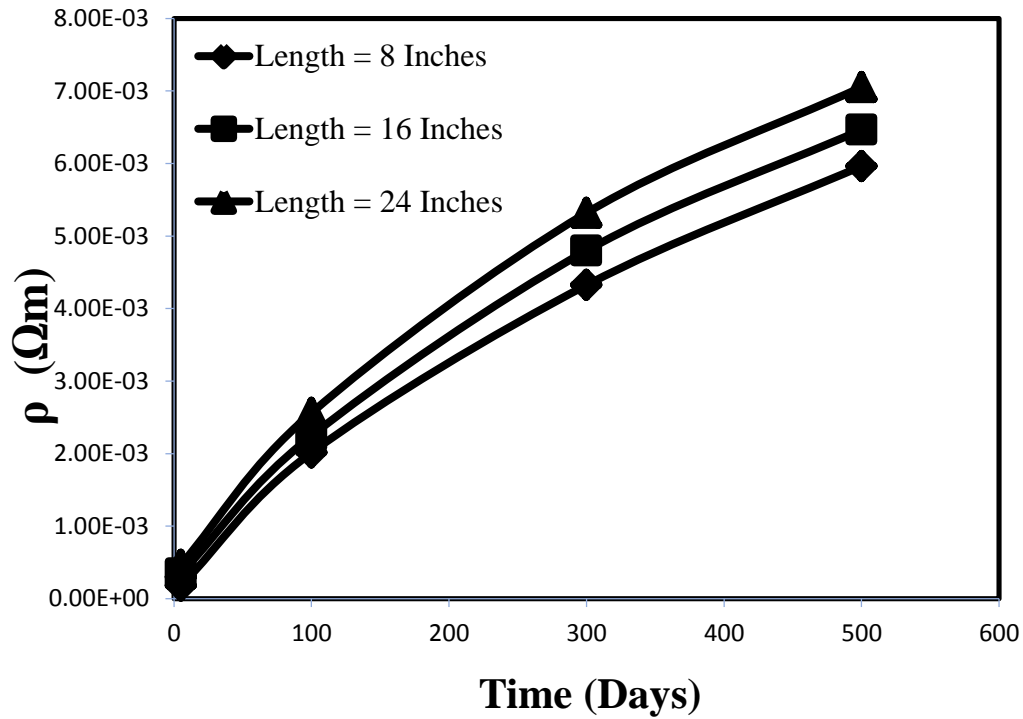


Figure 9. Variation of Electrical Resistivity in Steel with Time (500 Days) in 3.5% NaCl Solution

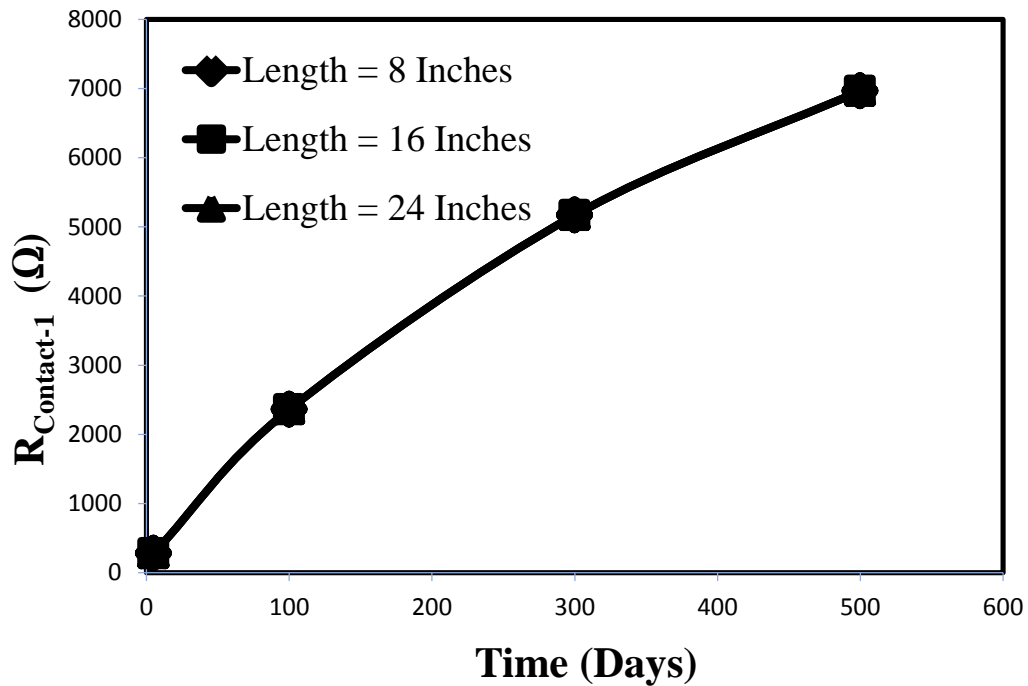


Figure 10. Contact Resistance of Contact 1 of the corroding steel specimen in 3.5% NaCl Solution

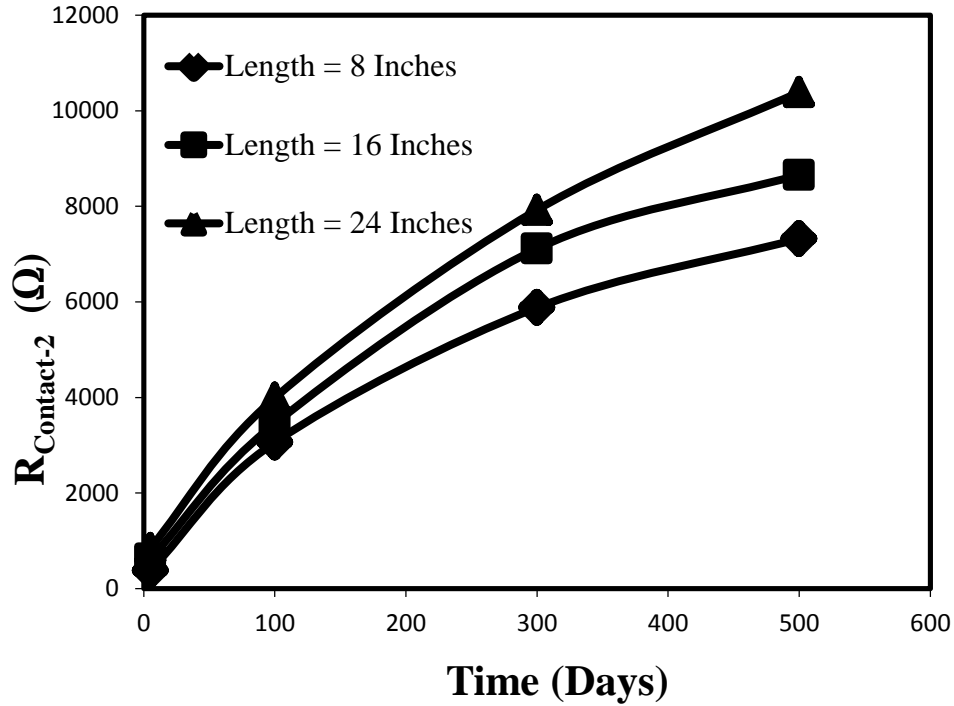


Figure 11. Contact Resistance of Contact 2 of the Corroding Steel Specimen in 3.5% NaCl Solution

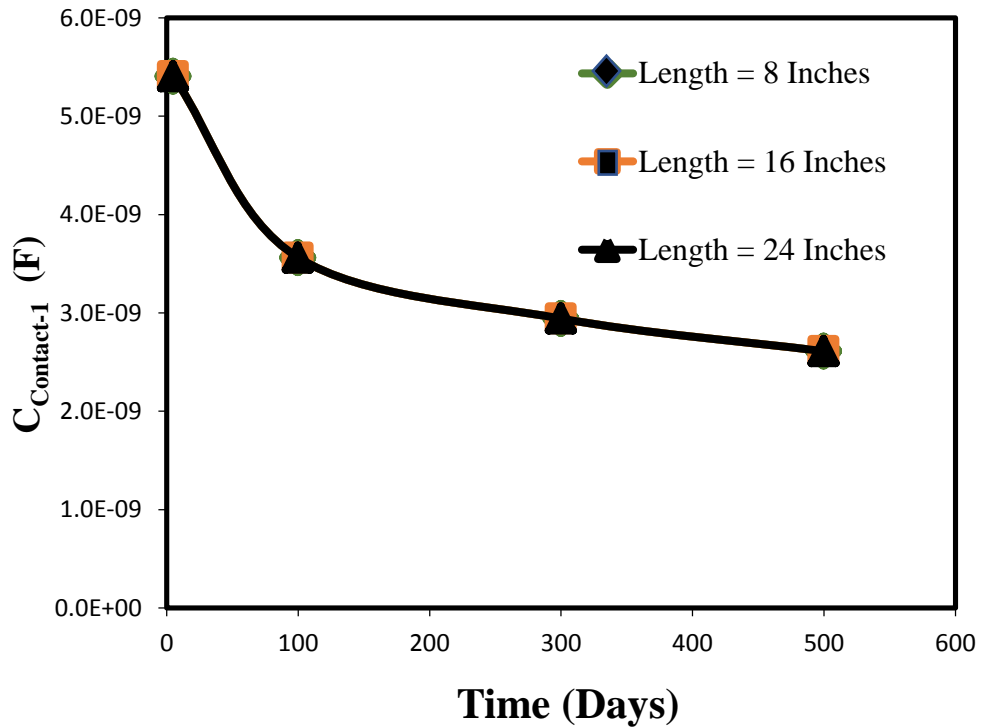


Figure 12. Contact Capacitance of Contact 1 of the Corroding Steel Specimen in 3.5 % NaCl Solution

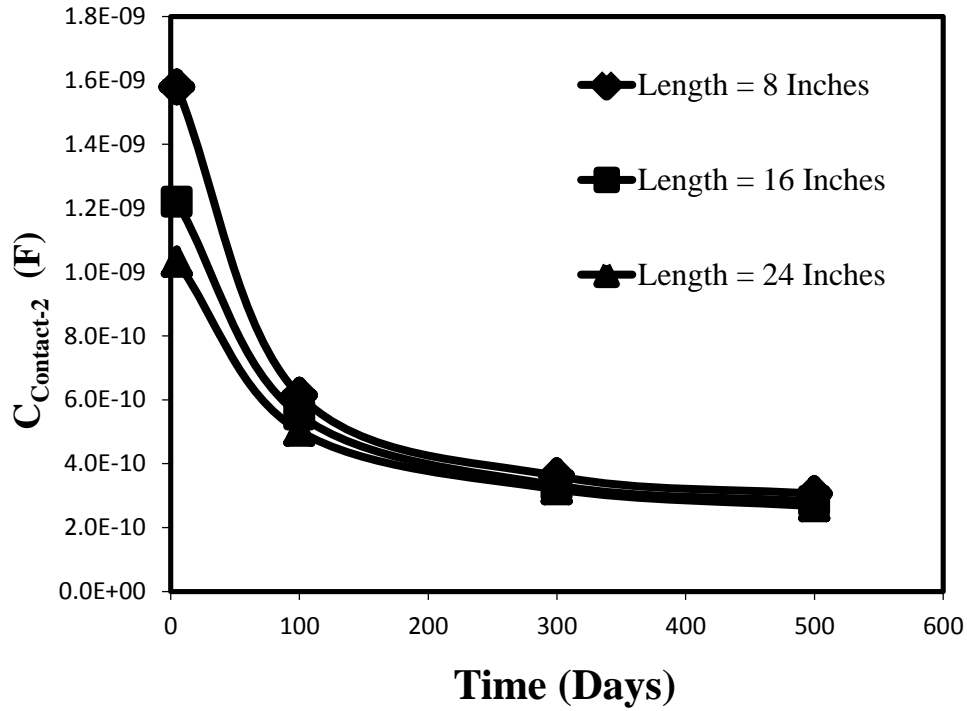


Figure 13. Contact Capacitance of Contact 2 of the Corroding Steel Specimen in 3.5% NaCl Solution

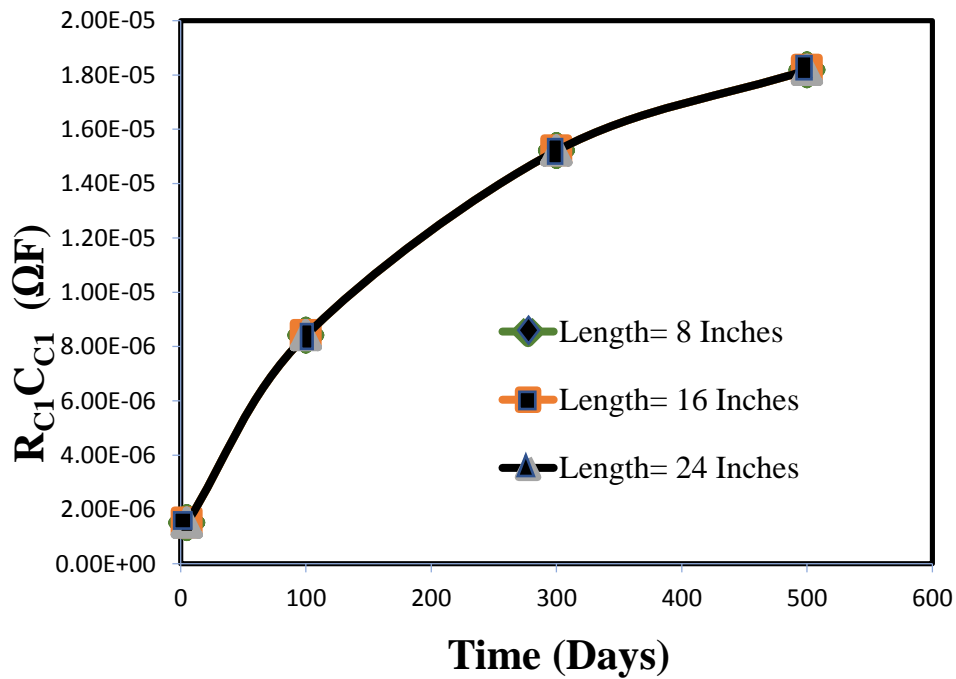


Figure 14. Variation of Electrical Corrosion Index $R_c C_c$ of Contact 1 of the Steel Specimen in 3.5 % NaCl Solution

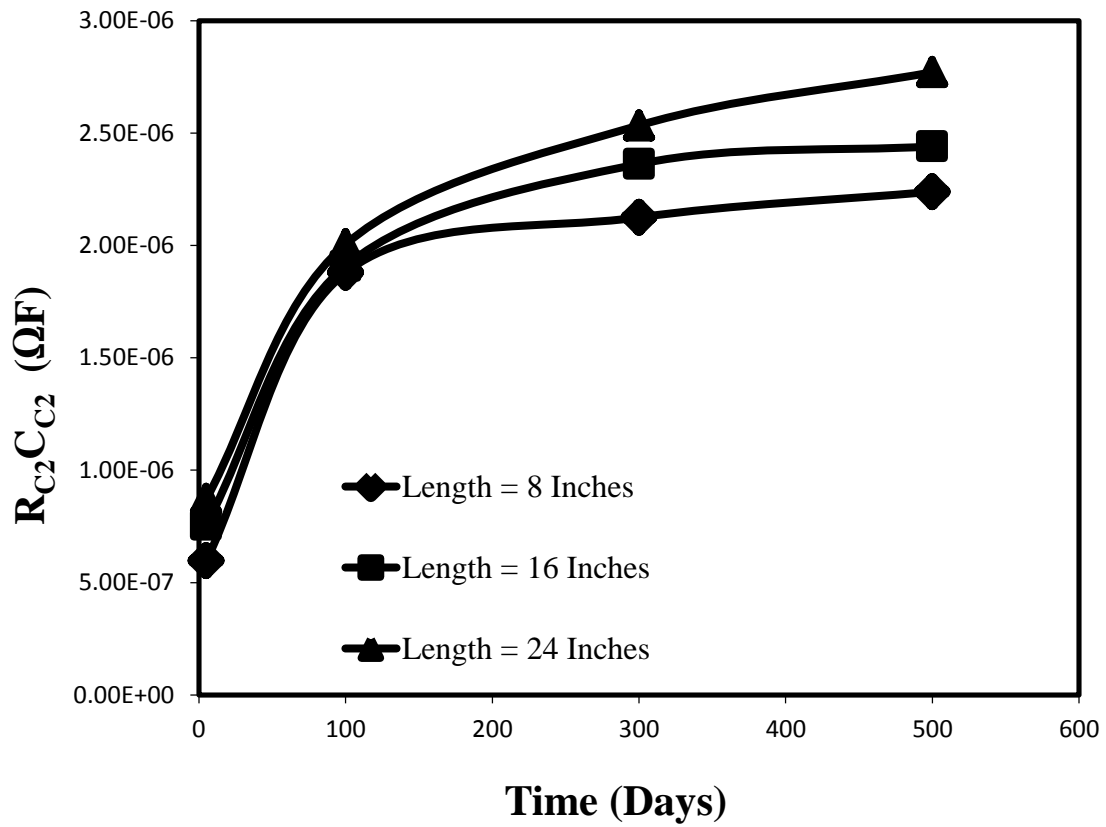


Figure 15. Variation of Electrical Corrosion Index R_cC_c at Contact 2 of the Steel Specimen in 3.5% NaCl Solution